Heavy-ion-induced desorption of organic molecules studied with Langmuir-Blodgett multilayer systems

R. Schmidt, Ch. Schoppmann, D. Brandl, A. Ostrowski, and H. Voit
Physikalisches Institut der Universität Erlangen-Nürnberg D-8520 Erlangen, Germany

D. Johannsmann and W. Knoll
Max-Planck-Institut für Polymerforschung Mainz D-6500 Mainz, Germany
(Received 29 May 1990)

Heavy-ion-induced desorption has been studied with samples consisting of Langmuir-Blodgett films made from Cd salts of fatty acids. The experiments confirm the result of previous works that heavy ions drill a crater into the sample surface. The explicit dependence of the crater depth on the electronic energy loss could be determined from the experiments. The craters exhibit the shape of a symmetric cone as obtained from a desorption model applied to the experimental data.

I. INTRODUCTION

Fast heavy ions with MeV energies are able to desorb intact organic molecules with high efficiency. This has been shown more than 15 years ago by Macfarlane and collaborators.[1] Meanwhile heavy ion induced desorption (HIID) mass spectrometry has become a useful tool for investigations of organic compounds in many laboratories. Parallel to this development, much effort has been spent to get a consistent picture of the desorption mechanism. It is well established that the electronic part of the primary-ion energy loss in the sample is responsible for desorption. In fact it has been shown, that the yield for secondary ions desorbed from a number of compounds is proportional to some power n of the electronic stopping power dE/dx, where n is a number between roughly 1 and 4.[2,3] Nevertheless, it is still not known in a fully microscopic frame how the electronic energy is transferred to the desorption degrees of freedom of the molecules. Most models treat this part of the desorption process more or less in a pure phenomenological way.

Many different and rather complicated steps can take place between energy deposition and the emission of the molecule from the sample. To shed light upon these processes, more elaborate experiments are needed in addition to those which already exist. In this context the use of dedicated samples becomes rather important. Langmuir-Blodgett (LB) films can be regarded as such samples because they represent a well-organized organic structure with great homogeneity and a thickness which can be tuned on the nm scale.[4] The present paper reports on HIID experiments performed with LB films. The aim of the experiments was to study (i) the crater formation proposed in Refs. 5 and 6, (ii) the dependence of the crater depth and the desorption depth (i.e., the maximum depth in the sample from which secondary ions are emitted) on the primary ion energy loss, (iii) the explicit shape of the craters, and (iv) the dependence of the secondary ion yield on the sample thickness. Similar experiments have been performed already in Refs. 5–8.

II. EXPERIMENTAL

Primary ions used for the present investigations were ^{16}O, ^{32}S, ^{63}Cu, and ^{127}I from the Erlangen EN tandem accelerator. Ion intensities did not exceed 300 particles per second. The sample was irradiated with typically 10^5-10^6 ions during the measurement. Due to the low beam dose the probability that a second primary ion hits an already irradiated spot on the sample is extremely small. Table I gives the energy E of the primary ions, the velocity v, and the energy loss dE/dx (as calculated with Bragg's rule from the tables of Ref. 9) in Cd stearate. The primary ion charge was identical with the equilibrium charge because the ions had to pass two foils thick enough to establish charge equilibrium (see Fig. 1).

Secondary ions desorbed from the LB films were detected by means of a time-of-flight (TOF) mass spectrometer which is shown schematically in Fig. 1. Primary ions pass the start detector (consisting of foil F2,

TABLE I. Energy E, velocity v, energy loss dE/dx, and desorption depth d of the primary ions. t is the crater depth obtained from the simple crater model of Ref. 5. τ and u are the crater depth and the crater width (measured at the surface) as calculated with the modified crater model. W_{0S} and W_{0A} are desorption probabilities for cdS and cdA, respectively, used in the latter model.

Primary ion	^{16}O	^{32}S	^{63}Cu	^{127}I
E (MeV)	5.4	12.1	19.0	45.5
v (cm/ns)	0.81	0.85	0.76	0.83
dE/dx (keV/nm)	1.3	2.4	3.5	5.8
d (nm)	15	20	30	>30
t (nm)	15	30	35	50
τ (nm)	10	20	30	>30
u (nm)	9	14	17	22
W_{0S}	0.50	0.70	0.87	0.99
W_{0A}	0.80	0.93	0.98	1.00

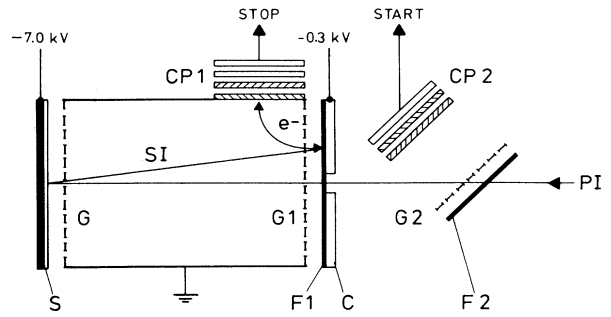

FIG. 1. Experimental set up. PI = primary ion, SI = secondary ion, S = sample. G, G1, G2 are grids; F1, F2 are thin Formvar foils. CP1, CP2 are channel plate detectors and C stands for converter plate.

grid G2, and channel plate detector CP2) and penetrate a hole in the converter plate C covered with the thin Formvar foil F1 before they hit the sample S. The sample is mounted on a target ladder which contains six additional samples, each of which can be positioned in front of the grid G without breaking vacuum. It should be noted that the primary ions impinge perpendicular to the sample surface. This is an important improvement compared to earlier investigations[5-8] because the experimental data can be explained much easier.

Desorbed ions are accelerated in the electric field between S and grid G and hit the foil F1 which is covered with CsI in order to enhance secondary electron emission. Secondary electrons produced by the impact of the secondary ions are accelerated between F1 and grid G1 and are bent into the channel plate detector CP1 by means of a magnetic field. CP1 yields the stop signal for the TOF measurement. The start signal is delivered by the secondary electrons which arise when the primary ions pass the foil F2. The detection efficiency of the start detector was determined to be 100%. The detection efficiency for secondary ions is not known;[10] it is estimated to be roughly 50% for the fatty acid molecules mainly investigated. Secondary ion yields quoted in this work are relative yields and are calculated from the ratio of stop to start signals.

LB films investigated were multilayer assemblies of Cd salts of fatty acids. The films were prepared at the MPI für Polymerforschung, Mainz. A Teflon trough was used for this purpose, which was positioned in a laminar flow box. Monolayer films were transferred from the subphase (milli-Q quality H_2O) to the substrate (microscope slides covered by 100 nm Au) by means of the dipping technique. The surface pressure π of the subphase was recorded by means of a Wilhelmy-type sensor. Transfer pressures π were 35 mN m^{-1} for Cd arachidate (cdA) and Cd stearate (cdS) and $\pi = 24.5$ mN m^{-1} for Cd palmitate (cdP), respectively. Transfer ratios were also recorded, they were close to 1 for all samples investigated. The subphase pH was adjusted by means of NaOH to a value of 6.5, the $CdCl_2$ concentration in the subphase was 8×10^{-4} M. The preparation of mixed assemblies consisting of different Cd salts was performed with great care in order to avoid any contamination of the layers (e.g., contamination of a cdS layer with cdA molecules). Finally it should be noted that only even numbers of layers could be deposited onto the substrate due to the hydrophobic character of the Au substrate.

The notation used below for the LB assemblies studied is explained for the following examples: 2cdA/$n$cdS denotes a film consisting of two layers of Cd arachidate covered by n layers of Cd stearate ($n = 2-12$, even). The cdA layers are deposited on the Au substrate (note the order). 8cdA/2cdS/2cdP denotes a film assembly consisting of eight layers of cdA (on the Au substrate) covered by two layers of cdS and additional two layers of cdP.

III. RESULTS

Figure 2 shows typical HIID mass spectra of negative ions desorbed by S and Cu ions from different 2cdA/$n$cdS samples. The dominant peak in the spectra belongs to the deprotonated stearic acid molecule $(S\text{-H})^-$. In some of the spectra $(A\text{-H})^-$ ions show up. The intensity of the $(A\text{-H})^-$ peak decreases for both primary ions with increasing number of cdS layers covering the cdA bilayer. The $(A\text{-H})^-$ intensity obtained for the same number of

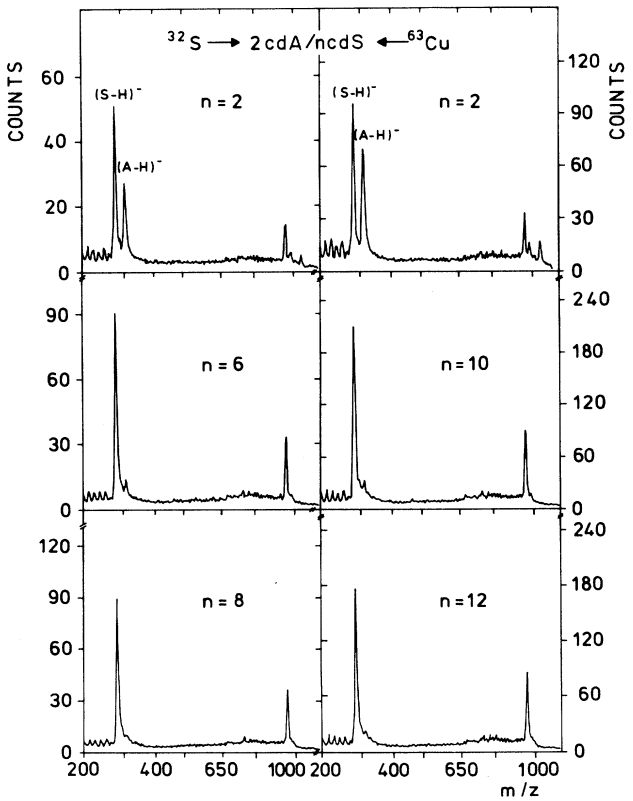

FIG. 2. ^{32}S (12.1 MeV) and ^{63}Cu (19.0 MeV) induced spectra of 2cdA/$n$cdS samples. n is the number of cdS layers. $(S\text{-H})^-$ and $(A\text{-H})^-$ denotes the deprotonated stearic acid and arachidic acid molecule, respectively.

cdS overlayers is larger for Cu ions than for S ions.

The fact that $(A\text{-H})^-$ ions are observed which stem from the bilayer on the bottom of the sample means that a crater is milled into the sample by the primary ion as proposed already in Refs. 5–8. The conclusion is stringent if one assumes that the LB film is close to defect free, that desorption from a protected layer is only possible if the molecules on top of this layer are removed and that diffusion of protected molecules to the sample surface is unlikely. These assumptions seem to be reasonable since a separate analysis of the same samples with the method of the spontaneous desorption[11] revealed only a very small number of defects (see below) and since model calculations on the basis of these assumptions reproduce—at least qualitatively—the observed data (see below).

^{32}S and ^{63}Cu primary ions differ in the amount of energy deposited in the samples (the ^{63}Cu energy loss exceeds the ^{32}S energy loss by a factor of 1.5, see Table I). Thus, the spectra of Fig. 2 indicate in addition that an energy loss dependent depth sensitivity exists for the MeV desorption from LB films, i.e., that the crater depth increases with increasing dE/dx. This finding is also supported by ^{16}O- and ^{127}I-induced data obtained from the same samples: the $(A\text{-H})^-$ peak disappears almost completely in the ^{16}O induced spectrum of the 2cdA/6cdS sample, it is still visible in the ^{127}I-induced spectrum with the thickest cdS overlayer investigated (2cdA/12cdS sample).

The depth sensitivity of the different primary ions in cdS films can be expressed in terms of the desorption depth d (depth from which desorption is still possible). The desorption depth for the different primary ions (different dE/dx values) investigated are given in Table I. d is also shown in Fig. 3 as a function of dE/dx. It should be noted that an error of the order of 2.5 nm has to be associated with the values given due to the bilayer structure of the samples. A function proportional to $(dE/dx)^{1/2}$ is also shown in Fig. 3 (solid line) because a $(dE/dx)^{1/2}$ dependence of the crater depth is proposed in Ref. 12.

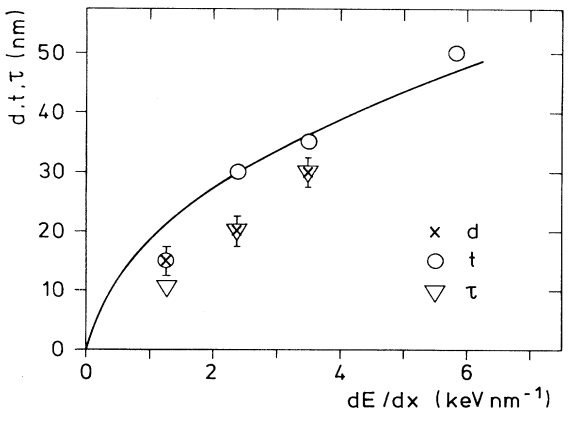

FIG. 3. Depth sensitivity d of the HIID for cdS films as a function of the energy loss dE/dx of the primary ions. t and τ are the crater depths obtained from a simple crater model and a modified crater model, respectively. The solid line is proportional to the square root of dE/dx.

The existence of a dE/dx dependent desorption depth can also be deduced from spectra obtained with ^{16}O (5.4 MeV) and ^{127}I (45.4 MeV) primary ions from 8cdP/2cdS/2cdA and 8cdA/2cdS/2cdP samples. The ^{16}O-induced spectra (see Fig. 4, left side) are dominated by the deprotonated fatty acid molecules desorbed from the bilayer on top of the sample. This indicates that the primary ion with small dE/dx is mostly sensitive to the sample surface. In the ^{127}I-induced spectra (see Fig. 4, right side) the deprotonated molecular ions from the 8 layers on the sample bottom are desorbed with large intensity.

Actually the $(P\text{-H})^-$ peak in the ^{127}I-induced spectrum of the 8cdA/2cdS/2cdP sample contains roughly the same number of counts as the $(A\text{-H})^-$ peak. This is due to the fact that the desorption probability for ions from Cd palmitate is larger (due to smaller binding energies) than for Cd arachidate. This is also the reason why the yield ratio for $(P\text{-H})^-$ to $(S\text{-H})^-$ ions exceeds the ratio for $(A\text{-H})^-$ to $(S\text{-H})^-$ ions in the ^{16}O-induced spectra shown in Fig. 4.

Obviously the measurements performed with the 2cdA/*n*cdS samples include the dependence of the HIID yield on the sample thickness. To deduce this dependence the $(S\text{-H})^-$ counts were normalized to the number of incident ions. The resulting yields Y are shown in Fig. 5 (triangles). The yields increase with increasing sample thickness till a maximum is reached; after this maximum a slight decrease is observed for still larger thicknesses.

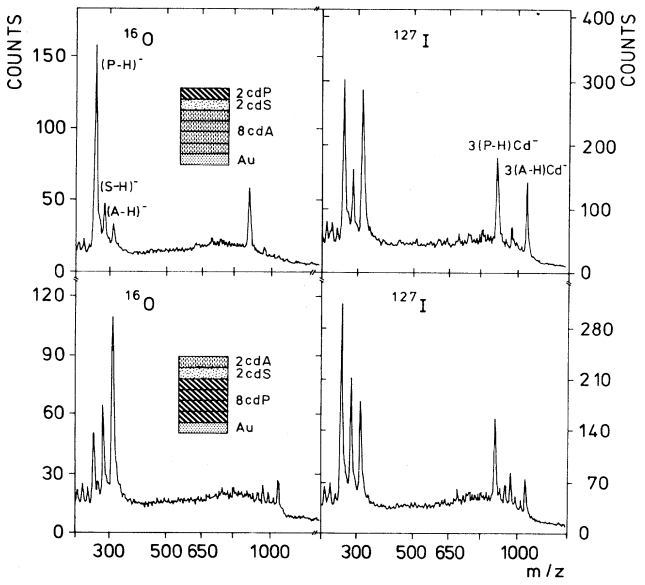

FIG. 4. ^{16}O (5.4 MeV) and ^{127}I (45.5 MeV) induced spectra of a 8cdA/2cdS/2cdP sample (upper part of the spectrum) and a 8cdP/2cdS/2cdA sample (lower part).

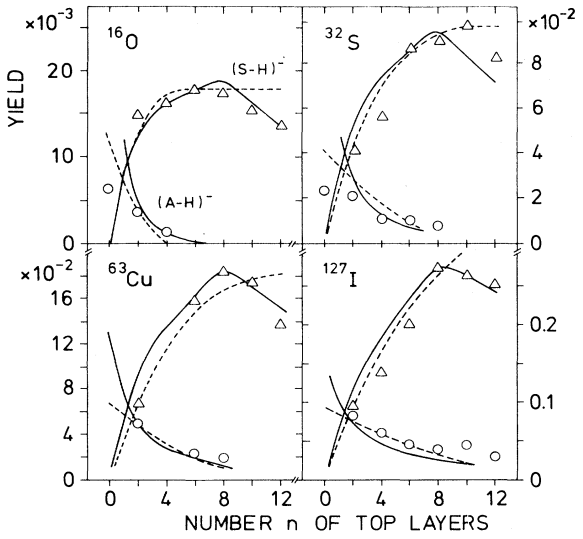

FIG. 5. Desorption yields for $(S\text{-H})^-$ ions (triangles) and $(A\text{-H})^-$ ions (circles) obtained for I, Cu, S, and O primary ions as a function of the number n of cdS layers. Dashed lines are fits with the simple crater model, solid lines are fits with the modified crater model.

The position of the maxima shifts to larger values of the sample thickness with increasing dE/dx of the primary ions. Similar features have been observed in the Kr-induced data for cdS samples[7] and for I-, S-, O-, and C-induced data for cdA samples.[8]

An increase of the $(S\text{-H})^-$ yield with increasing sample thickness must be correlated with a decrease of the $(A\text{-H})^-$ yield if the assumed crater formation is correct. Figure 5 shows that this is indeed the case (circles). The figure also demonstrates once more that the depth sensitivity of the HIID increases with increasing dE/dx of the primary ion.

IV. MODEL CALCULATIONS

The present investigations support the idea,[5,6] that a crater is milled into the LB film by the incident primary ion the depth of which increases with increasing dE/dx. If one makes the reasonable assumptions that a molecule from a deeper layer is not desorbed unless the molecules on top of it are removed and if one further assumes that the desorption probability W decreases below a value of 1 for some distance r measured from the primary ion track one obtains automatically a conelike shape for the crater. A cylindrical shape as assumed in Ref. 6 would result in a step function for the $(A\text{-H})^-$ yield curve.

If one assumes *a priori* that the crater formed by the heavy ion has the shape of a symmetric cone[5] one should get $(S\text{-H})^-$ and $(A\text{-H})^-$ ion yields (abbreviated Y_S and Y_A, respectively) for 2cdA/$n$cdS samples which are proportional to the volumes the $n$cdS top layers and the cdA bilayer occupy within the cone. Thus, one obtains the following expressions for the yield Y_S and Y_A, respectively,

$$Y_S \propto R^2 t \left[1 - \left[\frac{t-na}{t}\right]^3\right], \quad t \geq na ; \qquad Y_S \propto R^2 t, \quad t < na ; \tag{1}$$

$$Y_A \propto R^2 t \left[\left[\frac{t-na}{t}\right]^3 - \left[\frac{t-(n+2)a}{t}\right]^3\right], \quad t > na ; \qquad Y_A = 0, \quad t < na . \tag{2}$$

The quantities a, t, and R are the thickness of a LB monolayer (a was chosen to be 2.5 nm for the cdS and cdA molecules), the crater depth, and the cone radius, respectively. The measured dependence of the yields Y_S and Y_A on the number of cdS top layers can be fitted with the expressions given in the square brackets of Eqs. (1) and (2). The fits are shown in Fig. 5 (dashed lines). They allow to deduce the depths t of the craters milled into the sample by the different MeV heavy ions. The t values obtained are given in Table I and are shown as a function of dE/dx in Fig. 3 (circles). As expected, t increases with dE/dx in a similar way as the desorption depth d.

Absolute values for the cone radius R cannot be obtained in this model. From a comparison of the yields for different primary ions one can, however, deduce the ratios of the cone radii for different projectiles. These ratios agree reasonably well (considering the uncertainties in the t determination) with the ratios of the crater widths obtained in a more realistic model (see below).

The model predicts a saturation of the $(S\text{-H})^-$ yield for samples with a cdS thickness larger than the crater depth t. The ^{16}O-, and ^{32}S-induced data for which this criterion is fulfilled do not exhibit this behavior. Instead, a decrease of Y_S is observed for large n values. This indicates that the assumptions underlying this simple model are still too crude to describe the data also in detail.

Bolbach *et al.*[5] were the first who applied this simple model to fission fragment induced data. They got reasonable agreement between the model prediction and their data. This is somehow astonishing since one would only expect a crater with the shape of a symmetric cone if the primary ions hit the LB-film surface perpendicular (which was not the case in the experiments of Ref. 5).

We have also applied a more realistic model (called modified crater model in the following) for a comparison with our data. The model assumptions are (i) desorption of a protected molecule occurs only if the molecules on top of it are also desorbed, (ii) a cylindrical volume with radius 0.5 nm (fragmentation radius r_f) centered around the primary ion track does not contribute to the yield of unfragmented fatty acid ions, and (iii) the desorption probability W_i for ions originating from the ith layer (the $i=1$ layer is the monolayer on top of the sample, $i=1,2,\ldots,n$) depends on the distance r from the primary ion track in the following way:

$$W_i(r) = W_0 \exp[-U_0(i)/E(r)] . \tag{3}$$

$U_0(i)$ is the binding energy in the ith layer, W_0 the maximum desorption probability for a particular primary ion, and $E(r)$ the energy available for the desorption of a mol-

ecule at the distance r. $E(r)$ equals the energy density $e(r)$ deposited by δ electrons in a distance r perpendicular to the primary ion track multiplied by the volume of a fatty acid molecule; $e(r)$ was estimated according to the prescription given by Hedin *et al.*[13]

We allow U_0 to vary from layer to layer similar to the ansatz for a thermodesorption model made in Ref. 14 because it is known that different binding energies exist for molecules in different layers of a multilayer LB film.[14–16] One cannot expect that the desorption process is satisfactorily described by one particular binding energy.[17] This choice has of course the disadvantage that one is left with a large number of parameters (particularly if thick films are involved) even if U_0 is kept constant for successive bilayers as in the present calculations. To get, nevertheless, meaningful results one has to show that a number of independent measurements (e.g., Y_S and Y_A as a function of n measured for different impinging primary ions) can be reproduced simultaneously by the model calculations. Besides this, both magnitude and behavior of the $U_0(i)$ values obtained from the fit should be reasonable.

The contribution to the yields Y_S and Y_A from one layer is assumed to be proportional to the sum of the weighted areas of annular rings centered around the primary ion trajectory in a distance r_j. The energy density $e(r_j)$ is assumed to be constant within each particular ring. The weighting factor for each ring is the desorption probability $W_i(r_j)$ calculated according to Eq. (3). The total yield Y_S is obtained if the contributions from all n cdS layers are summed up:

$$Y_S \propto \sum_{j=1}^{J} \sum_{i=1}^{n} \left[\prod_{k=1}^{i} [W_{0S} \exp(-U_0(k)/E(r_j))] 2\pi r_j dr \right] . \tag{4}$$

The yield for $(A\text{-H})^-$ ions Y_A can be expressed as

$$Y_A \propto \sum_{j=1}^{J} W_{0S}(n,j) \{ W_{0A} \exp[-U_{0A}/E(r_j)] 2\pi r_j dr \} . \tag{5}$$

The quantities W_0 and $U_0(k)$ with additional indices S and A indicate the above-introduced maximum desorption probability and binding energy with respect to the stearic and arachidic acid molecules, respectively. $W_{0S}(n,j)$ is an abbreviation for the product occurring in Eq. (4), $r_j = r_f + (j - 1/2)D$ with r_f being the fragmentation radius (see above, $r_f = 0.5$ nm) and D the molecular diameter ($D = 0.5$ nm). The maximum r_j value r_J was chosen to be considerably larger than the range of δ electrons in the fatty acid samples (see Ref. 13).

Figure 5 shows the best fit curves (solid lines) to the experimental data using Eqs. (4) and (5) simultaneously with the same normalization constant. The binding energies obtained from these best fits are 0.70 eV for the cdA bilayer deposited on the Au substrate, 0.90 eV for the cdS bilayer on top of the cdA bilayer, and 0.87, 0.84, 0.81, 1.0, and 1.2 eV for the following double layers. The quality of the fits decreases only slightly if an average value of 0.86 eV is used for the first four bilayers on top of the cdA layers. It is, however, essential to use the relative large values of 1.0 and 1.2 eV for the topmost layers in order to reproduce the observed decrease of Y_S for $n > 8$. The values for the maximum desorption probabilities W_{0S} and W_{0A} used are given in Table I. They increase with increasing energy loss dE/dx of the projectiles.

Figure 6 gives an impression of the approximate shape of the craters milled into the LB films by the different primary ions. The figure shows cuts through the samples parallel to the primary ion trajectory. For each bilayer the outer boundary of the craters is determined by the arbitrary condition that the desorption probability $W_i(r)$ decreases for the first time below the value 0.2. It is obvious from the figure that both crater depth τ and crater width u (as measured at the sample surface) increase with increasing dE/dx of the incident ions; τ and u values are given in Table I.

The τ values are comparable with the values of the desorption depth d determined directly from the mass spectra (see Fig. 3). The squared crater radii are roughly proportional to the $(S\text{-H})^-$ yields obtained for different

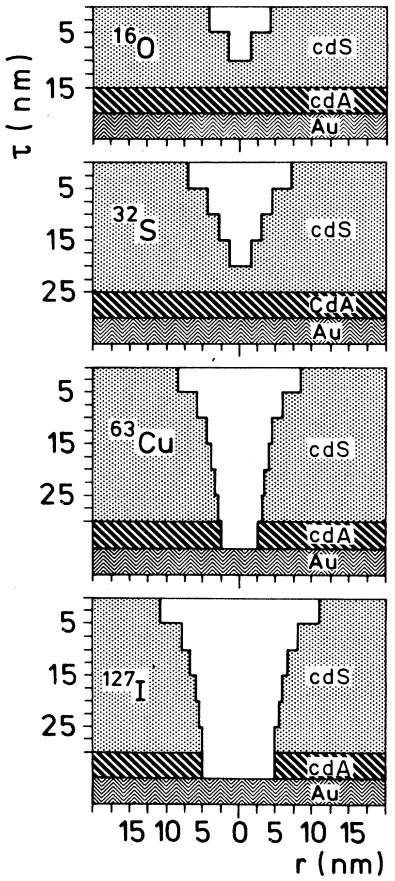

FIG. 6. Shape of the craters formed by ^{16}O, ^{32}S, ^{63}Cu, and ^{127}I primary ions in the 2cdA/*n*cdS samples as obtained from calculations with the modified crater model. For details see text.

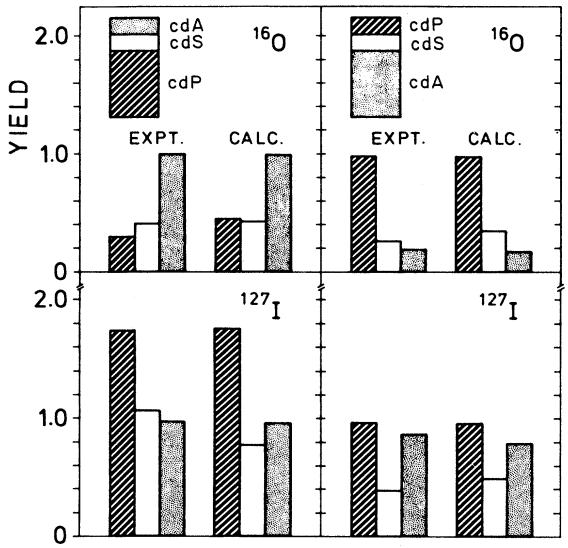

FIG. 7. Comparison between experimental yields for $(A\text{-H})^-$, $(S\text{-H})^-$, and $(P\text{-H})^-$ ions (displayed from right to left in the different histograms) desorbed by ^{16}O and ^{127}I primary ions from a 8cdP/2cdS/2cdA sample (left side) and a 8cdA/2cdS/2cdP sample (right side) with yields calculated by means of the modified crater model. Note that all yields are normalized to the experimental yields of the ions from the bilayer on top of the samples.

primary ions from the 2cdA/2cdS sample. This is what one expects for this sample: an increase of dE/dx increases in this case first of all the surface area from which desorption can occur.

The modified crater model was also applied to the spectra obtained from the 8cdA/2cdS/2cdP and 8cdP/2cdS/2cdA samples. Figure 7 shows a comparison between calculated and measured yields for $(P\text{-H})^-$, $(S\text{-H})^-$, and $(A\text{-H})^-$ ions. Obviously reasonable agreement can be obtained with the experimental data.

V. DISCUSSION

The mass spectra obtained from mixed layer LB assemblies contain molecular ions which stem from the protected layers [e.g., $(A\text{-H})^-$ ions in case of the 2cdA/$n$cdS samples]. This clearly shows that HIID is not only sensitive to the surface but also to the bulk of the sample, provided that one excludes (i) a possible diffusion of molecules from the protected layers to the surface prior to the primary ion bombardment, (ii) a contamination of the surface with these molecules as a result of a sloppy sample preparation, and (iii) a substantial defect structure (large unprotected areas) of the samples. The analysis of the samples investigated by means of the spontaneous desorption mass spectrometry[11] showed that these possibilities can be safely ruled out. If one further assumes that the ions in question cannot penetrate the top layers if these layers should remain intact after the primary ion impact one is led to the conclusion that a crater is milled into the LB film by the primary ion which extends all the way down to the protected layer. Crater formation has been proposed in Refs. 5 and 6 and is predicted in several theoretical models.[12,18,19]

The conclusion that a crater is formed is supported by the fact that a very simple crater model which assumes a conical shape for the crater as well as a more realistic modified crater model is able to reproduce the data qualitatively. The models account both for the decrease of Y for ions from protected layers and the increase of Y for ions from the top layers with increasing number n of these layers. Both models yield crater depths which increase with increasing primary ion energy loss and which agree reasonably with the desorption depth deduced directly from the mass spectra.

The modified model also allows one to deduce the approximate shape of the craters formed by the different projectiles (see Fig. 6). The craters have the shape of a symmetric cone with an aperture angle which decreases with increasing dE/dx and a crater width which increases with dE/dx. From the crater volumes obtained for the different primary ions one can calculate the number of molecules which are ejected by the impact of one primary ion. Most of these molecules are neutral.[20,21] If one uses values of 10^4 to 10^5 for the yield ratios of charged to neutral secondary particles (these values agree with ratios obtained for organic compounds in Ref. 21) one obtains indeed secondary ion yields which agree roughly with the measured values.

It is interesting to note that the absolute values of the binding energies $U_0(i)$ agree with values quoted in the literature. In Ref. 22 a value of 0.83 eV is found from thermodesorption experiments for a cdA monolayer on a hydrophilic substrate. The lower value of 0.7 eV for the cdA bilayer on the hydrophobic Au substrate obtained from our best fits seems therefore reasonable. Laxhuber *et al.*[15] and also Rabe[17] find an average U_0 for a cdA multilayer system of 0.83 eV with a slight decrease of U_0 with increasing number of layers. This compares nicely with the absolute values of U_0 and the decreasing tendency (with increasing film thickness) obtained from the present fits for LB samples with up to eight layers of cdS. The fact that U_0 for the topmost bilayer of the two thickest samples investigated had to be chosen significantly larger than the U_0 values of the layers underneath is in contrast to the finding of thermodesorption experiments.[15,17] The reason for this discrepancy is not clear. It might be due to the fact that the modified crater model is still too crude. It neglects, for instance, the effect reported by Rabe[17] that a particular layer becomes more tightly bound the more layers are put on top of it. This effect could be simulated by an increase of U_0 for the top layers of the thickest samples in the present model.

It is to be expected that crater formation occurs quite generally if organic and inorganic samples are bombarded with MeV heavy ions. The extension (depth and width) of the craters in the sample depends for a given projectile on the parameters of the sample (molecular binding energies, desorption probability, energy transfer from the projectile to the ions to be desorbed, etc.) as can be easily

shown in the framework of the crater models used in this work.

The desorption yield Y for ions from protected layers decreases with increasing number n of top layers (see Fig. 5). This decrease is more pronounced for primary ions with small electronic energy loss dE/dx, and thus demonstrates that a dE/dx dependent depth sensitivity exists in HIID. The desorption depths for different primary ions agree satisfactorily with the crater depths obtained with both models.

Samples with imperfect overlayers which exhibit channels (free of sample material) which extend down to the protected bilayer can, of course, obscure the depth determinations. A simple calculation shows, however, that the ratio between uncovered and covered area must exceed 1% before defects are able to influence the d determination (this was not the case according to a spontaneous desorption analysis[11]). In the calculation it is assumed that the primary ions (cross section $\approx 10^{-2}$ nm^2) hit the sample area (≈ 1 mm^2) in a completely statistical way (each 10^{-2}-nm^2 spot on the sample is hit only once by a primary ion due to the low ion dose). Besides this the following quantities enter into this calculation: the total number of primary ions impinging on the sample (typically 10^6), the minimum cross section of a cdS free channel (2×10^{-1} nm^2), a lower detection limit of 100 counts in the $(A\text{-H})^-$ ion peak and a neutral to charged species ratio of 10^5.

It should be noted that the yield for ions from the protected bilayer did not increase during the irradiation process. This is expected if the sample is irradiated with a very low ion dose as in the present case. It supports the premise that a spot on the sample hit once by a primary ion is not hit a second time.

VI. CONCLUSION

The present investigations indicate that conical craters are formed in LB films consisting of Cd salts of fatty acids if MeV ions hit these films. For a given sample both the depth and the width of the crater depends on the electronic energy loss of the MeV ion. A heavy ion with a large dE/dx value drills a deeper hole (with an almost cylindrical shape) into the sample than a light ion with small dE/dx. This means that HIID possesses a certain depth sensitivity (from 10 to >30 nm in case of the samples and projectiles investigated in this work) which can be adjusted choosing the appropriate projectiles. As a result of the crater formation one obtains a dependence of the desorption yield on the sample thickness. The yield increases with the sample thickness till a maximum is reached for a thickness which equals approximately the crater depth.

[1]D. F. Torgerson, R. P. Sworonski, and R. D. Macfarlane, Biochem. Biophys. Res. Commun. **60**, 616 (1974).
[2]H. Voit, E. Nieschler, B. Nees, R. Schmidt, Ch. Schoppmann, P. Beining, and J. Scheer, J. Phys. (Paris) Colloq. **50**, C2-237 (1989); D. Brandl, R. Schmidt, Ch. Schoppmann, A. Ostrowski, and H. Voit, Phys. Rev. B **43**, 5253 (1991).
[3]P. Hakansson and B. Sundqvist, Rad. Eff. **61**, 179 (1982).
[4]G. G. Roberts, Adv. Phys. **34**, 475 (1985).
[5]G. Bolbach, S. Della-Negra, C. Deprun, Y. LeBeyec, and K. G. Standing, Rapid Commun. Mass Spectrom. **1**, 22 (1987).
[6]G. Säve, P. Hakansson, B. U. R. Sundqvist, R. E. Johnson, E. Söderström, S. E. Lindqvist, and J. Berg, Appl. Phys. Lett. **51**, 1379 (1987).
[7]G. Bolbach, R. Beavis, S. Della-Negra, C. Deprun, W. Ens, Y. LeBeyec, D. E. Main, B. Schueler, and K. G. Standing, Nucl. Instrum. Methods Phys. Res. B **30**, 74 (1988).
[8]G. Säve, P. Hakansson, B. U. R. Sundqvist, E. Söderström, S. Lindqvist, and J. Berg, Int. J. Mass Spectrom. Ion Proc. **78**, 259 (1987).
[9]L. C. Northcliffe and R. F. Schilling, Nucl. Data Tables Sec. A **7**, 233 (1970).
[10]P. Dück, W. Treu, H. Fröhlich, W. Galster, and H. Voit, Surf. Sci. **95**, 603 (1980).
[11]R. Schmidt, B. Nees, Ch. Schoppmann, D. Brandl, A. Ostrowski, H. Voit, D. Johannsmann, and W. Knoll, Thin Solid Films **195**, 307 (1991).
[12]I. S. Bitensky, A. M. Goldenberg, and E. S. Parilis, J. Phys. (Paris) Colloq. **50**, C2-213 (1989).
[13]A. Hedin, P. Hakansson, B. Sundqvist, and R. E. Johnson, Phys. Rev. B **31**, 1780 (1985).
[14]L. A. Laxhuber and H. Möhwald, Surf. Sci. **186**, 1 (1987).
[15]L. A. Laxhuber, B. Rothenhäusler, G. Schneider, and H. Möwald, Appl. Phys. A **39**, 173 (1986).
[16]J. P. Jones and G. M. Webby, Thin Solid Films **178**, 211 (1989).
[17]J. P. Rabe, Thin Solid Films **159**, 359 (1988).
[18]R. E. Johnson, B. U. R. Sundqvist, A. Hedin, and D. Fenyö, Phys. Rev. B **40**, 49 (1989).
[19]E. R. Hilf and H. F. Kammer, J. Phys. (Paris) Colloq. **50**, C2-245 (1989).
[20]M. Salehpour, P. Hakansson, B. Sundqvist, and S. Widdiyasekera, Nucl. Instrum. Methods B **13**, 278 (1986).
[21]B. Nees, thesis, University Erlangen-Nürnberg, Erlangen, 1988 (unpublished).
[22]L. A. Laxhuber and H. Möhwald, Langmuir **3**, 837 (1987).